

# Low-distortion, high-strength bonding of thermoplastic microfluidic devices employing case-II diffusion-mediated permeant activation†

Thomas I. Wallow,‡ Alfredo M. Morales,\* Blake A. Simmons, Marion C. Hunter, Karen Lee Krafcik, Linda A. Domeier, Shane M. Sickafoose, Kamlesh D. Patel and Andy Gardea

Received 4th July 2007, Accepted 31st August 2007

First published as an Advance Article on the web 19th September 2007

DOI: 10.1039/b710175a

We demonstrate a new method for joining thermoplastic surfaces to produce microfluidic devices. The method takes advantage of the sharply defined permeation boundary of case-II diffusion to generate dimensionally controlled, activated bonding layers at the surfaces being joined. The technique is capable of producing bonds that exhibit cohesive failure, while preserving the fidelity of fine features in the bonding interface. This approach is uniquely suited to production of layered microfluidic structures, as it allows the bond-forming interface between plastic parts to be precisely manipulated at micrometre length scales. Distortions in microfluidic device channels are limited to the size scale of the permeant-swollen layer; 6  $\mu\text{m}$  deep channels are routinely produced with no detectable cross-sectional distortions. Conventional thermal diffusion bonding of identical parts yields less strongly bonded microfluidic structures with increasingly severe dimensional compressions as bonding temperatures approach the thermoplastic glass-transition temperature: a preliminary rheological analysis is consistent with the observed compressions. The bond-enhancing procedure is easily integrated in standard process flows, uses inexpensive reagents, and requires no specialized equipment.

## Introduction

Microfluidic fabrication continues to employ a relatively invariant suite of methods for bonding thermoplastics, such as acrylics, poly(carbonates), and cyclic olefin copolymers (COCs). A series of recent reviews<sup>1</sup> distinguishes several categories of methods for bonding similar thermoplastic surfaces: thermal diffusion bonding (TDB), pressure-induced sealing, thermal lamination, adhesive bonding, conventional solvent bonding, and laser welding. Additional methods adapted from joining of macroscopic plastic parts<sup>2</sup> are reported on some occasions. Recent innovations include the use of solvent bonding coupled with sacrificial fill materials to preserve channel dimensions,<sup>3</sup> a spin-on phase-compatible COC lamination layer,<sup>4</sup> microwave bonding,<sup>5</sup> and plasma surface modification prior to TDB.<sup>6</sup> For COCs, such as Zeonor™ or Topas™ specifically, TDB is employed nearly exclusively.<sup>7,8</sup> Current COC bonding methods frequently suffer from limitations, including channel blockage, channel distortion, poor bond strength and durability, and inhomogeneous channel surface properties.

Glassy polymers typically display case-II diffusion when exposed to selected permeants.<sup>9</sup> In this diffusive process, a permeant-laden zone forms at the polymer–permeant interface and advances into the glassy polymer linearly with time:

Sandia National Laboratories, P.O. Box 969, Livermore, CA, 94551-0969, USA. E-mail: amorale@sandia.gov; Fax: +1-925-294-3410; Tel: +1-925-294-3540

† Electronic supplementary information (ESI) available: Results and discussion supplementary information with table and figure. See DOI: 10.1039/b710175a

‡ Current address: Advanced Micro Devices, One AMD Place, Sunnyvale, CA 94088, USA.

a sharply defined boundary separates the swollen layer from the unpermeated glassy core. The process has been subjected to extensive experimental studies, particularly for poly(methyl methacrylate)<sup>10</sup> and poly(styrene),<sup>11</sup> and increasingly sophisticated theoretical descriptions continue to be developed.<sup>12</sup> Swelling by the permeant allows increased polymer chain movement, that in turn results in greater plasticity and a decreased glass transition temperature in the permeated layer.<sup>13</sup> Depending on the strength of the given polymer–permeant interaction, the process may be arrested following permeation, resulting in a stable plasticized matrix, or proceed to ultimate dissolution of the polymer.

We have carried out studies to characterize case-II diffusion of solvent mixtures into Zeonor™ and have used that information to rationally develop a new approach to COC bonding. Fig. 1 illustrates the case-II-mediated bonding approach. One or both pieces to be joined are immersed in a medium (liquid or vapor) that promotes case-II permeation. A swollen layer forms at a rate that can be controlled by medium composition, immersion time, and temperature. No polymer dissolution occurs during immersion. Following immersion, the parts are aligned and joined in a heated press. We employ permeant compositions whose case-II front propagation velocities can be varied precisely and systematically to produce well-defined, activated, permeant-swollen bonding interfaces in which interchain entanglements may occur at markedly lower temperatures ( $\Delta T \sim 30$  °C for the process demonstrated here) than required for TDB. Zeonor™ microfluidic channels bonded in this manner fail cohesively at pressures in excess of 1900 psi. In contrast, TDB produces channels with significant to extreme cross-sectional distortion and results in adhesive failures at pressures approaching 1000 psi.

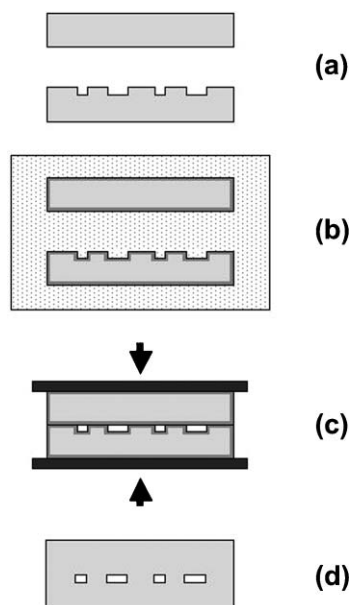


**Fig. 1** Schematic of a case-II enhanced bonding process. (a) Plastic microfluidic parts to be joined. (b) Timed immersion of parts in a medium that promotes case-II permeation into the plastic. (Permeated zone not shown to scale.) (c) Joining of the surface-permeated parts in a heated press. (d) Final joined part.

## Experimental

Zeonor™ 1060R (manufacturer specified  $T_g = 100\text{ °C}$ ) was obtained from Nippon Zeon Chemicals in injection-molded plaque and pellet forms. All chemicals were obtained in analytical grades and used without additional purification. The general plastic microfluidic fabrication process used in this study has been described in previous publications.<sup>8</sup> Briefly, fabrication of polymer microfluidic devices involves the creation of a master etched in silicon or glass; plating of the master to produce a nickel stamp; large-lot replication of the microfluidic substrate by injection molding; and precision sealing of the substrate against a drilled Zeonor™ plaque lid. Optical interferometry scans of injection molded substrates have shown the substrates to deviate less than  $0.2\text{ }\mu\text{m}$  from the original master and faithfully replicate artifacts of the master fabrication process, such as sloped channel sidewalls.<sup>8</sup> Pre-bonding nominal dimensions reported in this paper were obtained from optical interferometry of substrates, not from cross-sections.

### Case-II diffusion in Zeonor™ 1060R

**Bulk Case-II permeation studies.** Zeonor™ sheets (1.6 mm thick; approximately  $25 \times 25\text{ mm}$  coupon size) were rinsed with acetone and isopropanol and allowed to air-dry overnight. Sheets were immersed in 80 : 20 wt% ethanol : decalin mixture containing 0.5 wt% iodine as a staining agent; stainless steel wires threaded through small drilled holes were used to suspend the coupons in the liquid. Prior to immersion, the ethanol : decalin solution was placed in a thermostatted bath at  $20 \pm 0.1\text{ °C}$  and allowed to equilibrate for several hours before measurements were initiated. All bulk permeation studies and quartz crystal microbalance (QCM) experiments

were conducted with the solvent mixture at  $20\text{ °C}$  only, as this temperature is close to the average temperature in a standard laboratory chemical hood.

**Quartz crystal microbalance studies of Zeonor™ swelling and dissolution.** Interactions of Zeonor™ 1060R films with solvent mixtures and vapours were studied using a modified, commercially available compensated phase-locked oscillator (CPLO)-equipped QCM (RQCM, Maxtek Corporation, Cypress, CA, USA). The CPLO is used along with extensions of standard QCM physical models<sup>14</sup> to help resolve difficulties associated with lossy films and to facilitate analysis of processes occurring during swelling and dissolution.<sup>15</sup>

Solvent bonding with pure decalin was initially tried but resulted in complete collapse of 70 micron deep microfluidic channels. Bonding with pure decalin was extremely difficult to characterize as decalin is a good solvent for Zeonor™ and immersion in decalin results in both rapid permeation and rapid dissolution. The deep gel layer that formed after immersion in decalin was extremely soft and distortable and attempts to rinse off excess decalin resulted in gross distortions to microfluidic channels. Attempts to measure diffusivity constants of pure decalin into Zeonor™ using the QCM method were unsuccessful due to the immeasurably fast penetration of decalin into the Zeonor™ thin films. Thus, only ethanol : decalin mixtures were studied in detail.

Zeonor™ films were prepared by dissolving injection-molded Zeonor™ 1060R stock in decalin, cineole, or mixtures of the two. Thin films were spin-cast on gold-electrode coated AT-cut quartz crystals with nominal fundamental resonant frequencies of 5 MHz. Following coating, the Zeonor™ films ( $0.325 \pm 0.005\text{ }\mu\text{m}$  thickness) were baked in air at  $180\text{ °C}$  for 10 min. Film thickness characterization of witness pieces by profile analysis of white-light interferometric scans (Wyko NT 3300 Profiling System, Veeco, Tucson, AZ, USA) indicated that highly reproducible, striation-free films are produced under the spin-casting conditions employed. Coated wafers were mounted in immersion holders. Covered glass containers filled with solutions of interest were placed in a thermostatted bath at  $20 \pm 0.1\text{ °C}$  and allowed to equilibrate for several hours. Samples were introduced and measurements were immediately initiated. Solutions were stirred using a teflon-coated stir bar.

**Microscopic sample examination.** Bulk permeation samples and actual bonded microfluidic devices were prepared for cross-sectional observation as follows. A Buehler Isomet low-speed diamond saw was used to section near the area of interest. The sections were then mounted in low temperature epoxy encapsulant (Epofix, Struers Inc., Cleveland, OH, USA). All mounts were placed in a pressure bomb at 200 psi overnight. In the case of actual bonded microfluidic devices, the pressure bomb helped fill the microfluidic channels with epoxy prior to full cure and prevented channel collapse during the grinding and polishing steps. During cure, temperature exotherms of up to  $70\text{ °C}$  are observed for similar procedures. The mounts were hand-ground to the area of interest, placed in a sample holder, and then processed further using a Struers Abrapol 2 polisher. Initial grinding employed serial one

minute treatments with 600, 1200, and 4000 grit SiC paper at 150 N. Samples were ultrasonically cleaned in water and dried. Samples were next polished using 3  $\mu\text{m}$  water-soluble diamond in an alcohol lubricant (DP-Blue, Struers Inc., Cleveland, OH, USA). Fine polishing was carried out using first a silk cloth, then a suede cloth. Samples were again ultrasonically cleaned and dried prior to final polishing using a velvet cloth and a 0.06  $\mu\text{m}$  colloidal silica solution to produce a defect-free surface.

Optical examinations and measurements were carried out using a Nikon MM-40 measuring microscope configured with a CCD video camera interfaced to a workstation using Metronics Inc. QC-5000 metrology software. An alternate Leitz Orthoplan microscope configured with a CCD camera interfaced to a workstation using standard image capture and manipulation software was used in some instances.

### Bonding processes

**Thermal diffusion bonding.** A standard process is carried out as follows: The surfaces to be bonded are rinsed with acetone, then blown dry with a nitrogen stream. Coupons are then baked in an oven at 45  $^{\circ}\text{C}$  for approx. 1 h to remove residual solvents. The two coupons are mated and Kapton tape is applied to the perimeter, covering the bond line. The mated coupons are placed between preheated pressure plates and the assembly is inserted between preheated (30 min; 88  $^{\circ}\text{C}$ ) platens of a Carver press. The assembly is loaded at 350 psi for 45 min. The press is cooled with running water ( $\sim 10$  min) to less than 27  $^{\circ}\text{C}$ ; the bonded coupon is removed. Bonding at 99  $^{\circ}\text{C}$  is carried out in an analogous manner.

**Case-II bonding using ethanol : decalin infusion.** A standard process is carried out as follows: the surfaces to be bonded are rinsed with acetone, then blown dry with a nitrogen stream. Coupons are then baked in an oven at 45  $^{\circ}\text{C}$  for approx. 1 h to remove residual solvents. In a covered Petri dish, the drilled plaque lid is immersed in an 80 : 20 wt% mixture of ethanol : decalin for 15 min at 21  $^{\circ}\text{C}$ . Following infusion, the plaque lid is dipped in a Petri dish containing pure ethanol, then rinsed with fresh ethanol from a wash bottle. The piece is blown dry with a nitrogen stream. The patterned coupon is treated similarly, but the decalin : ethanol infusion time is limited to 30 s. The two coupons are mated and Kapton tape is applied to the perimeter, covering the bond line. The mated coupons are placed between pressure plates and the assembly is inserted between the platens of a Carver press. The platens are adjusted until the top platen just touches the top of the assembly; at this point, the press is heated to 60  $^{\circ}\text{C}$  over the course of 15 min. Following heating, the assembly is loaded at 180 psi for 20 min. The press is cooled with running water ( $\sim 10$  min) to less than 27  $^{\circ}\text{C}$ ; the bonded coupon is removed. Since residual decalin vapors can be detected after bonding, bonded coupons are then baked in an oven at 53  $^{\circ}\text{C}$  overnight. The same infusion bonding method is used to produce microfluidic chips by bonding four inch diameter Zeonor<sup>TM</sup> wafers with a variety of channel depths and channel spacings.

**Pressure testing.** Failure pressures were measured on bonded channels (dimensions: 10 mm (*l*)  $\times$  1 mm (*w*)  $\times$  70  $\mu\text{m}$  (*d*))

accessed through precision-drilled plaque lids. In one series of tests, either of two Senstronics pressure sensors (1450 or 5800 psi; 0.5 and 2 psi resolution, respectively, Senstronics Ltd., UK) were attached to capillaries *via* Sandia National Laboratories' CapTite<sup>TM</sup> fittings.<sup>16</sup> Fittings were attached to the test structure inlets and outlets and glued into place using an epoxy resin (3 M Scotch-Weld Epoxy Adhesive DP-460 cured 2.5–3 days at 57  $^{\circ}\text{C}$ ). A stepper motor syringe pump capable of reaching pressures of 1800 psi was attached to the inlet of the structure being measured. Water was fed through the structure until it dripped from the outlet continuously to verify the total replacement of any air with water. The outlet was then attached to the pressure sensor *via* CapTite<sup>TM</sup> fittings. Pressure sensor output was monitored at 1 Hz using the LabVIEW software program.

For high-strength bonds, a similar assembly of CapTite<sup>TM</sup> fittings was used to connect channels to a Jasco PU-980 reciprocating HPLC pump capable of reaching pressures of 6000 psi. Water was fed through the structure until it dripped from the outlet continuously to verify the total replacement of any air with water. The outlet was then sealed using a polyetherimide NanoPort<sup>TM</sup> cap (Upchurch Scientific, Oak Harbor, WA, USA). Pressures were controlled in manual increments and monitored using an analog pressure transducer. Pressure sensor output was monitored using the LabVIEW software program.

### Viscoelasticity of Zeonor<sup>TM</sup> 1060R

**Dynamic mechanical analysis of Zeonor<sup>TM</sup>.** A TA Instruments Q800 Dynamic Mechanical Analysis (DMA) tool was employed for static and dynamic measurements. Zeonor<sup>TM</sup> coupons were machined to approximately 35  $\times$  12.9  $\times$  1.9 mm dimensions and fixtured for measurements using standard sample mounts. Precise dimensional measurements were carried out on each coupon prior to analysis. Storage and loss moduli were measured as a function of both temperature and frequency at 0.04% maximum strain. Stress relaxation measurements at constant strain were carried out as static measurements at selected temperatures using a strain of 0.05%. Strain evolution measurements at constant stress were carried out as static measurements at selected temperatures with an applied stress of 0.04 MPa.

## Results and discussion

### Case-II permeation in Zeonor<sup>TM</sup> 1060R

We have demonstrated the existence of case-II mediated permeation in Zeonor<sup>TM</sup> by two independent methods. The first is adapted directly from pioneering studies of case-II diffusion in PMMA.<sup>9</sup> The technique employs an iodine stain to enhance visualization of the case-II swelling front in bulk Zeonor<sup>TM</sup> sheets and allows determination of the bulk case-II front velocity. The second method uses a QCM approach to confirm the linear permeant mass uptake with time characteristics of case-II diffusion. QCM experiments are also used to measure thin-film case-II front velocities and equilibrium permeant uptakes for a series of permeant mixtures.

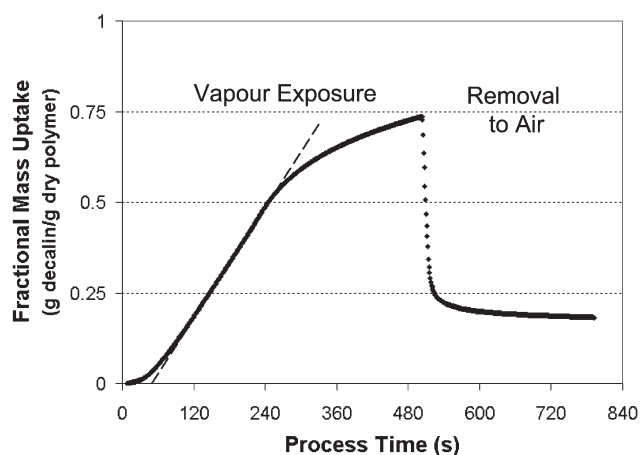


**Fig. 2** Decalin vapour uptake and loss from a  $0.325\ \mu\text{m}$  thick Zeonor<sup>TM</sup> film at  $20\ ^\circ\text{C}$ . Removal from vapour-saturated chamber results in rapid loss of decalin followed by trapping of approximately  $0.2\ \text{g per g}$  residual decalin in the film.

The detailed results and analysis for the case-II permeation studies are reported in the ESI.† At  $20\ ^\circ\text{C}$ , the average permeation front velocity  $v_0$  for an  $80 : 20\ \text{wt}\%$  mixture of ethanol : decalin is  $0.15\ \mu\text{m min}^{-1}$ . Thus, immersion of Zeonor<sup>TM</sup> into this permeant mixture is convenient for implementing a bonding process: approximately  $1\ \mu\text{m}$  of Zeonor<sup>TM</sup> is permeated per 7 min of immersion time.

### Bonding processes

The demonstration of a successful, two-layer Zeonor<sup>TM</sup> infusion bonding process was rationally guided by understanding the case-II permeation of ethanol : decalin mixtures but still required considerable development work. Permeant composition, permeation depth, bonding temperature, bonding pressure, and ancillary rinse and drying steps were explored systematically. Vapour infusion bonding was explored as well, but showed less reproducible bonding behavior. The preferred method for bonding resulting from these studies uses a 10 min long immersion (approximately  $1.8\ \mu\text{m}$  deep infusion according to the QCM data) of pre-drilled plaque lids produced by immersion in an  $80 : 20\ \text{wt}\%$  ethanol : decalin mixture and a brief 30 s dip of the patterned injection molded substrate in the

same solution. In the absence of the dip treatment, poor bonding is observed. Surface resistance to solvent absorption has been described in a related COC.<sup>17</sup> We infer that this effect may account for poor bonding, but have not explored the issue in detail. We hypothesize that the surface resistance was also responsible for the poor reproducibility of the vapour infusion experiments.

We anticipated that variations in post-infusion processing would adversely affect bonding reproducibility. In practice, this is not observed. When a QCM-monitored  $0.325\ \mu\text{m}$  thick Zeonor<sup>TM</sup> film is exposed to a saturated decalin vapor, anomalous but case-II predominant permeation occurs (Fig. 2). If the film is removed to air, rapid loss of approximately 75% of the absorbed decalin occurs in seconds, followed by a sharp transition to a much slower mass loss regime. Approximately  $0.2\ \text{g decalin per g Zeonor}^{\text{TM}}$  remains trapped in the film for at least an hour, (although actual capillary electrophoresis and dielectrophoresis chips bonded with this technique have been used for a month and have not been affected by residually trapped decalin). This behavior is highly reproducible and indicates the formation of a surface resistance layer or rapid vitrification of the plasticized Zeonor<sup>TM</sup> matrix as decalin evaporates. We postulate that the consistent concentration of trapped decalin remaining in the Zeonor<sup>TM</sup> results in reproducible bonding performance and significant process latitude. In any case, this observation suggests that the equilibrium permeant uptake measured by QCM is unlikely to reflect the concentration of permeant present at the interface during bonding. An experiment more directly comparable to the case-II bonding process that immerses the film in liquids is difficult to interpret due to frequency shifts associated with multiple liquid immersions, rinsing, drying, and evaporation.

In order to explore trade offs between feature fidelity and bond strength achievable by TDB, two bonding temperatures were investigated:  $88\ ^\circ\text{C}$  was chosen as a temperature likely to produce devices with tolerable distortions and  $99\ ^\circ\text{C}$  (essentially at  $T_g$  of Zeonor<sup>TM</sup> 1060) was chosen as a temperature likely to provide high bond-strength parts. Relative to TDB, conditions used to bond infusion-treated Zeonor<sup>TM</sup> employ lower temperature ( $60\ ^\circ\text{C}$ ) and reduced pressure (180 psi). Microfluidic channel dimensions are preserved with superior fidelity as a result. The optical micrographs shown in Fig. 3

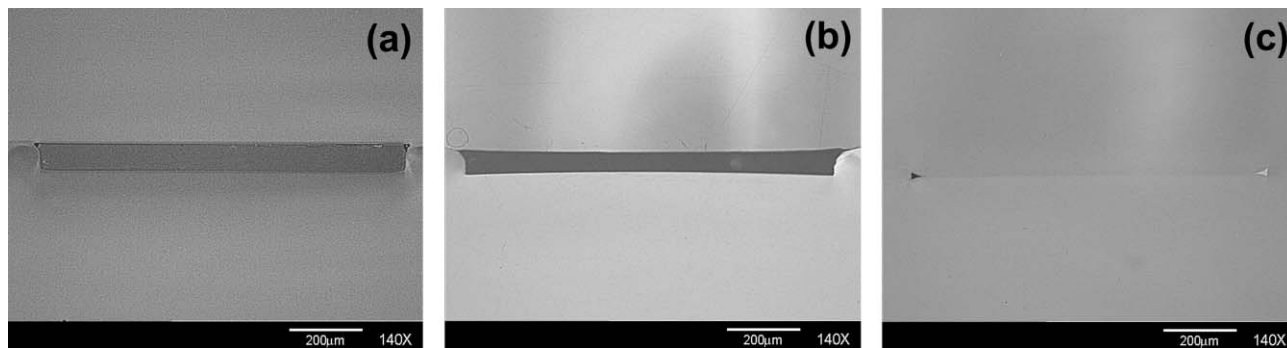


**Fig. 3** Optical micrographs showing cross-sections of  $1\ \text{mm} \times 70\ \mu\text{m}$  microfluidic channels prepared using (a) case-II enhanced bonding, (b) thermal bonding at  $88\ ^\circ\text{C}$ , and (c) thermal bonding at  $99\ ^\circ\text{C}$ . (a) Channel depth is uniformly  $70 \pm 2\ \mu\text{m}$ ; (b) compressed mid-channel depth is  $53 \pm 2\ \mu\text{m}$ ; (c) almost complete channel occlusion occurs.

**Table 1** Failure of bonded channels under pressure<sup>a</sup>

Bonding method	Failure pressure/psi	Failure mechanism
TDB, 88 °C	930–1000	Adhesive
TDB, 99 °C	600–1000	Adhesive
Infusion, 60 °C	1900–2340	Cohesive

<sup>a</sup> A minimum of 3 samples per bonding condition were tested.

illustrate both the feature fidelity possible by bonding with an 80 : 20 wt% ethanol : decalin mixture and the channel compression resulting from TDB. Infusion-based solvent bonding at 60 °C produces cross-sections whose dimensions are indistinguishable from those of the injection molded substrate prior to bonding. At 88 °C, TDB results in significant vertical compression; at the channel midpoint, channel depth is reduced by 25%, and both lid and base are noticeably bowed. At 99 °C, TDB results in nearly complete channel occlusion.

Pressure test results are summarized in Table 1. The case-II bonding method approximately doubles channel failure pressure relative to TDB bonding. Failed channels were inspected by optical microscopy to determine the mode of failure. Delamination propagating along the bondline (adhesive failure) is easily distinguishable from channel rupture that does not propagate along the bondline (cohesive failure). Based on the observed channel collapse and adhesive failure, TDB samples never successfully bonded.

We have encountered significant experimental difficulties in consistently forming strong bonds between Zeonor™ surfaces and fittings needed to pressurize the microfluidic channel. For case-II bonded samples in particular, ruptures are frequently observed at or near the fittings at 1900–2000 psi. A mid-channel rupture occurred in one sample at 2340 psi; tests in which rupture occurs in mid-channel are considered to be most representative of actual bond strength.

Infusion-bonded Zeonor™ failure pressures are comparable to those reported for PMMA structures fabricated using a solvent bonding process enhanced by a sacrificial channel fill compound.<sup>3</sup>

The infusion bonding method allows successful fabrication of otherwise challenging plastic microfluidic structures. Fig. 4 illustrates successful fabrication of a nominally 6.1 μm deep inlet particle filter shelf within a microfluidic channel. Analysis of the cross-sections reveals no detectable bowing across the length of the shelf; the measured shelf depth is  $5.6 \pm 0.5 \mu\text{m}$ . Fig. 4c shows a nominally 6 μm deep flow-restriction channel in cross-section. The channel shows only minor distortion and is fully functional.

The infusion bonding method has been successfully used to produce microfluidic chips by bonding four inch diameter Zeonor™ wafers with a variety of channel depths and channel spacings (Fig. 5a). Preliminary microscopy on the failed infusion bonded chips after pressure testing show that the nucleated crack originates at the side of the channel but quickly propagates into the bulk Zeonor™ (Fig. 5b and 5c). In contrast, TDB samples delaminate along the bond line when tested under pressure.

Capillary electrophoresis microfluidic chips produced *via* infusion bonding have been successfully used to separate molecular species and fluorescein isothiocyanate labeled

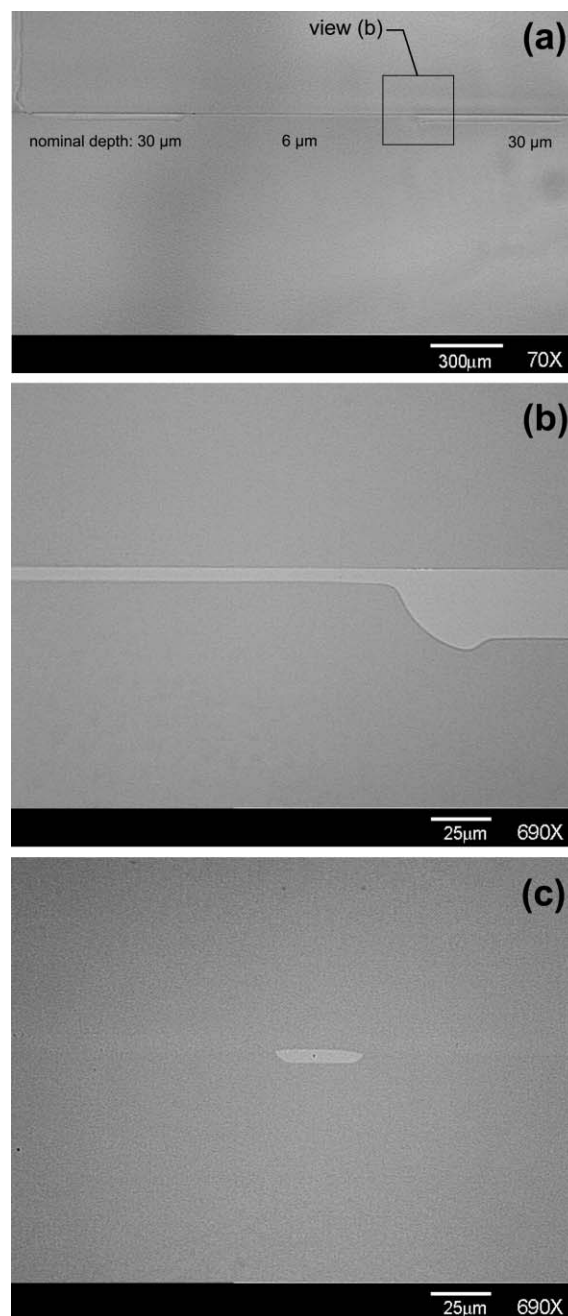


**Fig. 4** Optical micrographs showing cross-sections of shallow channel features. (a) and (b) show a particle filter shelf. The shelf is  $980 \mu\text{m}$  ( $l$ )  $\times$   $1000 \mu\text{m}$  ( $w$ ) and  $5.6 \pm 0.5 \mu\text{m}$  deep. (c) shows a  $5.2 \pm 1 \times 35.8 \pm 1 \mu\text{m}$  flow-restriction channel. Nominal channel dimensions are given in the text.

proteins. Similarly bonded chips have been used in insulator based dielectrophoresis experiments for the selective trapping of polymer microbeads.<sup>18</sup>

#### **Zeonor™ viscoelasticity under thermal bonding conditions**

Results of a series of dynamic and static mechanical analysis tests are summarized in Table 2. Bonding in a press approximates constant stress conditions. Zeonor™ strain response at constant stress exhibits qualitatively and quantitatively

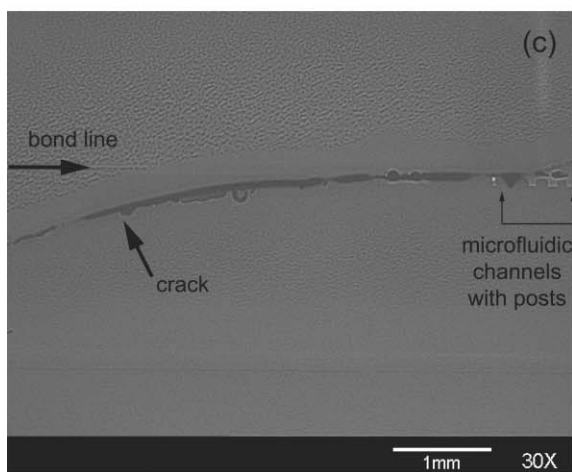
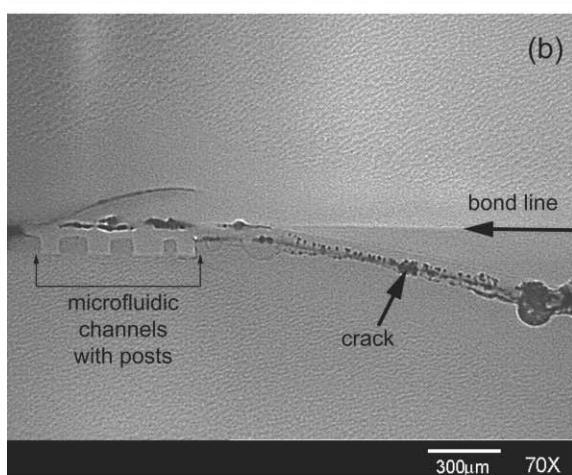
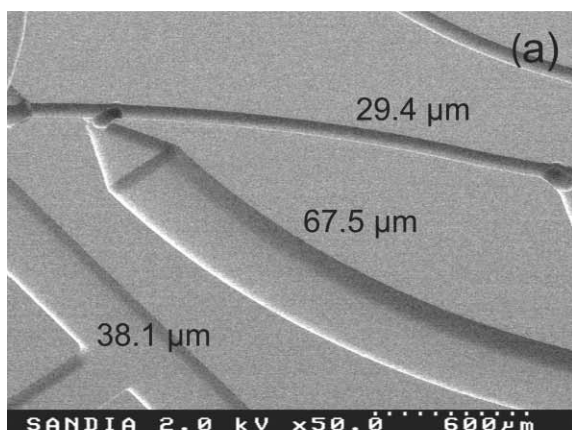


**Fig. 5** (a) SEM photograph showing different channel sizes on a Zeonor™ wafer prior to bonding. Channel depths are annotated. (b) and (c) are optical micrograph cross-sections of an infusion bonded channel with posts after failing under pressure testing. The cracks on both sides of the fluidic channel propagate into the bulk of the Zeonor™.

different behaviours at 88 °C and 99 °C. At 88 °C, total strain  $\epsilon_{(\text{tot})}$  reaches a limiting value within 10 min of stress application. Upon stress release following a 20 min stress application, residual strain  $\epsilon_{(\text{res})}$  is approximately 0.005%. At 99 °C,  $\epsilon_{(\text{tot})}$  increases continuously with time. Upon stress release following a 20 min stress application,  $\epsilon_{(\text{res})}$  is

**Table 2** Static and dynamic mechanical analysis of Zeonor™ 1060R under TDB conditions

	$\epsilon_{(\text{tot})}$ (%) <sup>a</sup>	$\epsilon_{(\text{res})}$ (%) <sup>a</sup>	Freq./Hz	E'/GPa <sup>b</sup>	E''/MPa <sup>b</sup>	$t_c$ /s <sup>c</sup>
T = 88 °C	0.0075 <sup>d</sup>	0.005	0.1	1.8	140	87
			1	1.7	100	
			10	1.7	70	
T = 99 °C	0.32 <sup>e</sup>	0.32	0.1	0.85	400	19
			1	1.3	250	
			10	1.5	130	

<sup>a</sup> Constant stress at 0.04 MPa. <sup>b</sup> At specified frequency; 0.04% strain. <sup>c</sup> Stress decay curves fit to data as  $\sigma(t) = a - be^{(-t/t_c)}$ , where  $a$ ,  $b$ , and  $t_c$  are constants; 0.05% strain. <sup>d</sup> Plateau value at  $t > 10$  min. <sup>e</sup> Continuous strain increase at  $\sim 0.016\%$  per min observed;  $\epsilon_{(\text{tot})}$  value at  $t = 20$  min reported.

approximately 0.32% and indicates that significant softening and creep of the polymer is occurring at this temperature.

Values for Zeonor™ storage ( $E'$ ) and loss ( $E''$ ) moduli at TDB temperatures obtained from dynamic mechanical analysis show frequency dependence. We take low-frequency values as the most appropriate for correlating with bonding results. Decreased  $E'$  and increased  $E''$  at 99 °C reflect the softening also observed under constant-stress conditions.

Static tensile stress relaxation measurements display the anticipated exponential stress decay:<sup>19</sup> characteristic times for relaxation are 87 s and 19 s at 88 °C and 99 °C, respectively. In both cases, characteristic times are quite short relative to bonding process time.

Taken as a whole, these measurements are consistent with the observation of modest plastic distortions at temperatures where Zeonor™ thermal bonding becomes feasible, and progressively more severe distortions as bonding temperatures approach  $T_g$ . Viewed in conjunction with pressure tests of bonded channels (Table 1), these findings suggest that neither TDB condition suffices for producing low-distortion, high-strength bonds in Zeonor™. More quantitative correlation between Zeonor™ viscoelasticity at bonding temperatures and observed bonding deformation will require a significantly expanded rheological analysis. Note that since infusion bonding affects only the surface of Zeonor™, at this time we do not have the tools needed to measure the viscoelastic constants of the solvent treated polymer.

## Conclusions

We have demonstrated a new polymer microfluidic bonding method that is uniquely capable of producing low-distortion, high-strength bonds in Zeonor™ 1060R. The method takes advantage of the characterization of case-II diffusion in Zeonor™ to produce an activated, controlled bonding interface. Permeant infusion from an 80 : 20 wt% mixture of ethanol : decalin enables a robust bonding process that yields microfluidic channels with high-strength and dimensional fidelity. The infusion bonding method uses inexpensive reagents and equipment and is easily integrated in standard bonding process flows. Further development of this bonding method will allow the fabrication of multilayer Zeonor™ microfluidic devices.

Glass-based microfluidic manufacturing has long enjoyed significant advantages over plastic manufacturing, and has thus been favored for use in complex integrated analysis systems, such as the  $\mu$ ChemLab developed at Sandia National Laboratories, USA.<sup>20</sup> The infusion bonding method presented here allows plastics-based manufacturing of challenging structures that were previously achievable only in glass manufacturing, thus providing a further step toward lower cost manufacturing platforms.

## Acknowledgements

We would like to thank Dr LeRoy Whinnery for invaluable help in fixturing CapTite<sup>TM</sup> fittings. Dr Andrew Vance is gratefully acknowledged for proof reading the final draft. Sandia BioBriefcase and LIGA teams are gratefully acknowledged for support in all aspects of polymer microfabrication. Funding by the US Department of Homeland Security Office of Research and Detection Development Program is acknowledged. Sandia is a multiprogram laboratory operated by Sandia Corporation, a Lockheed Martin Company, for the United States Department of Energy's National Nuclear Security Administration under contract DE-AC04-94AL85000.

## References

- 1 H. Becker and C. Gaertner, *Electrophoresis*, 2000, **21**, 12; A. de Mello, *Lab Chip*, 2002, **2**, 31N; E. Verpoorte and N. F. de Rooij, *Proc. IEEE*, 2003, **91**, 930.
- 2 J. Rotheiser, *Joining of Plastics*, Hanser, Munich, 2nd edn, 2004.
- 3 R. T. Kelly, T. Pan and A. T. Woolley, *Anal. Chem.*, 2005, **77**, 3536.
- 4 F. Bundgaard, T. Nielsen, D. Nilsson, P. Shi, G. Perozziello, A. Kristensen and O. Geschke, *Spec. Publ. -R. Soc. Chem.*, 2005, **297**(2), 372.
- 5 K. F. Lei, S. Ahsan, N. Budraa, W. J. Li and J. D. Mai, *Sens. Actuators, A*, 2004, **114**, 340.
- 6 Z. Wu, N. Xanthopoulos, F. Reymond, J. S. Rossier and H. H. Girault, *Electrophoresis*, 2002, **23**, 782; C. H. Ahn, J.-W. Choi, G. Beauchage, J. H. Nevin, J.-B. Lee, A. Puntambekar and J. Y. Lee, *Proc. IEEE*, 2004, **92**, 154; D. Nikolova, E. Dayss, G. Leps and A. Wutzler, *SIA Surf. Interface Anal.*, 2004, **36**, 689.
- 7 *Micro Total Analysis Systems 2003*, ed. M. A. Northrup, K. F. Jensen and D. J. Harrison, Transducers Research Foundation, San Diego, 2003, vol. 1–2; *Micro Total Analysis Systems 2004*, ed. T. Laurell, J. Nilsson, K. Jensen, D. J. Harrison and J. P. Kutter, Royal Society of Chemistry, Cambridge, 2004 vol. 1–2.
- 8 B. A. Simmons, B. Lapizco-Encinas, R. Shediach, J. Hachman, J. Chames, J. Brazzle, J. Ceremuga, G. Fiechtner, E. B. Cummings and Y. Fintschenko, *Spec. Publ. -R. Soc. Chem.*, 2005, **297**(2), 171; P. Mela, A. van den Berg, Y. Fintschenko, E. B. Cummings, B. A. Simmons and B. J. Kirby, *Electrophoresis*, 2005, **26**, 1792; A. M. Morales, J. D. Brazzle, R. W. Crocker, L. A. Domeier, E. B. Goods, J. T. Hachman, C. K. Harnett, M. C. Hunter, S. S. Mani, B. P. Mosier and B. A. Simmons, *Proc. SPIE-Int. Soc. Opt. Eng.*, 2005, **5716**, 89.
- 9 T. Alfrey, Jr., E. F. Gurnee and W. G. Lloyd, *J. Polym. Sci., Part C: Polym. Symp.*, 1966, **12**, 249; A. H. Windle, in *Polymer Permeability*, ed. J. Comyn, Elsevier Applied Science, London, 1985, ch. 3, pp. 75–118.
- 10 N. Thomas and A. H. Windle, *Polymer*, 1978, **19**, 255; N. Thomas and A. H. Windle, *Polymer*, 1981, **22**, 627; N. Thomas and A. H. Windle, *Polymer*, 1982, **23**, 529; G. C. Sarti, C. Costoli and S. Masoni, *J. Membr. Sci.*, 1983, **15**, 181.
- 11 A. S. Michaels, H. J. Bixler and H. B. Hopfenberg, *J. Appl. Polym. Sci.*, 1968, **12**, 991; C. H. M. Jacques and H. B. Hopfenberg, *Polym. Eng. Sci.*, 1974, **14**, 441; C. H. M. Jacques and H. B. Hopfenberg, *Polym. Eng. Sci.*, 1974, **14**, 449; R. C. Lasky, E. J. Kramer and C.-Y. Hui, *Polymer*, 1988, **29**, 673; T. P. Gall and E. J. Kramer, *Polymer*, 1991, **32**, 265.
- 12 A. El Afif and M. Grmela, *J. Rheol.*, 2002, **43**, 591; A. S. Argon, R. E. Cohen and A. C. Patel, *Polymer*, 1999, **40**, 6991; D. A. Edwards, *J. Polym. Sci., Part B: Polym. Phys.*, 1996, **34**, 981.
- 13 N. A. Peppas, J. C. Wu and E. D. Von Meerweil, *Macromolecules*, 1994, **27**, 5626.
- 14 S.-W. Lee, W. D. Hinsberg and K. K. Kanazawa, *Anal. Chem.*, 2002, **74**, 125.
- 15 W. Hinsberg, F. A. Houle, S.-W. Lee and K. Kanazawa, *Macromolecules*, 2005, **38**, 1882.
- 16 <http://www.ca.sandia.gov/pubs/factsheets/captiteSAND2003-8556P.pdf>.
- 17 T. B. Nielsen and C. M. Hansen, *Ind. Eng. Chem. Res.*, 2005, **44**, 3959.
- 18 A. M. Morales, B. A. Simmons, T. I. Wallow, K. J. Campbell, S. S. Mani, B. Mittal, R. W. Crocker, E. B. Cummings, R. V. Davalos, L. A. Domeier, M. C. Hunter, K. L. Krafcik, G. J. McGraw, B. P. Mosier and S. M. Sickafoose, *Proc. SPIE-Int. Soc. Opt. Eng.*, 2006, **6109**, 10901.
- 19 R. S. Lakes, *Viscoelastic Solids*, CRC Press, Boca Raton, 1999, pp. 5 and 6.
- 20 R. F. Renzi, J. Stamps, B. A. Horn, S. Ferko, V. A. VanderNoot, J. A. West, R. Crocker, B. Wiedenman, D. Yee and J. A. Fruetel, *Anal. Chem.*, 2005, **77**, 435; J. A. Fruetel, R. F. Renzi, V. A. VanderNoot, J. Stamps, B. A. Horn, J. A. West, S. Ferko, R. Crocker, C. G. Bailey, D. Arnold, B. Wiedenman, W.-Y. Choi, D. Yee, I. Shokair, E. Hasselbrink, P. Paul, D. Rakestraw and D. Padgen, *Electrophoresis*, 2005, **26**, 1144.